

# Universal Superfluid Transition and Transport Properties of Two-Dimensional Dirty Bosons

Giuseppe Carleo,<sup>1</sup> Guilhem Boéris,<sup>1</sup> Markus Holzmann,<sup>2,3</sup> and Laurent Sanchez-Palencia<sup>1</sup>

<sup>1</sup>Laboratoire Charles Fabry, Institut d'Optique, CNRS, Univ Paris Sud 11,

2 avenue Augustin Fresnel, F-91127 Palaiseau cedex, France

<sup>2</sup>LPTMC, UMR 7600 of CNRS, Université Pierre et Marie Curie, 75005 Paris, France

<sup>3</sup>Université Grenoble I/CNRS, LPMMC, UMR 5493, B.P. 166, 38042 Grenoble, France

(Received 13 May 2013; published 2 August 2013)

We study the phase diagram of two-dimensional, interacting bosons in the presence of a correlated disorder in continuous space, by using large-scale quantum Monte Carlo simulations at finite temperature. We show that the superfluid transition is strongly protected against disorder. It remains of the Berezinskii-Kosterlitz-Thouless type up to disorder strengths comparable to the chemical potential. Moreover, we study the transport properties in the strong disorder regime where a zero-temperature Bose-glass phase is expected. We show that the conductance exhibits a thermally activated behavior vanishing only at zero temperature. Our results point towards the existence of a Bose *bad-metal* phase as a precursor of the Bose-glass phase.

DOI: 10.1103/PhysRevLett.111.050406

PACS numbers: 05.30.Jp, 02.70.Ss, 67.25.dj, 72.15.Rn

Transport properties in quantum materials are governed by a complex interplay of disorder and interactions. While disorder tends to localize particles, interactions may strongly alter the single-particle picture by either reinforcing or suppressing localization. Dramatic effects are expected in two dimensions (2D), such as metal-insulator transitions [1–3], suppression of superfluidity [4–8], and presumably high- $T_c$  superconductivity [9]. Possible phase transitions are, however, particularly elusive owing to the absence of true long-range order even in extended phases [10,11], and many questions remain open. For instance, resistance measurements in Si-MOSFETs suggest a metal-insulator transition [1], which may be attributed to quantum localization or classical percolation [2], but experiments on GaAs heterostructures point towards a crossover behavior [3]. Studies of the superfluid Berezinskii-Kosterlitz-Thouless (BKT) transition [12,13] have also been reported for  $^4\text{He}$  films adsorbed on porous media [4,5]. While the BKT transition is unaffected in the weak disorder limit [14], the question of its relevance for strong disorder is left open owing to the difficulty to identify a universal jump of the superfluid density [6–8]. Moreover, a question that is attracting much debate is whether many-body localization effects [15–19] can drive a finite-temperature metal-insulator transition in two dimensions.

Ultracold quantum gases in controlled disorder offer a unique tool to address these questions in a unified way [20]. In clean or disordered quasi-2D geometries, direct consequences of vortex pairing [21], superfluidity [22], quasi-long-range phase coherence [23,24], and resistance measurements [25] have been reported. On the theoretical side, most knowledge relies on lattice models with uncorrelated disorder [26–31]. Conversely, little is known when the disorder is continuous, is correlated, and can sustain a classical percolation threshold. An important class of such models is the one realized by optical speckle potentials used in recent ultracold-atom experiments [32–36].

In this Letter, we report on an *ab initio* path-integral quantum Monte Carlo study of the phase diagram of interacting 2D bosons in the presence of a speckle-type disorder. We show that, although the density profile exhibits large spatial modulations, the superfluid BKT transition is strongly protected against disorder. This holds up to disorder strengths comparable to the chemical potential, where the zero-temperature Bose-glass transition is expected. The critical properties of the *dirty* superfluid transition can be understood in terms of a universal description including a simple renormalization of the critical parameters. In particular, we find that the superfluid transition occurs while the fluid percolates with a density significantly above the critical density of the clean system. It allows us to rule out the classical percolation scenario. Moreover, we study the conductance by means of a novel quantum Monte Carlo estimator. Deep in the strong disorder regime, we find direct evidence of an insulating behavior, characterized by a conductance that decreases with temperature. Our data are consistent with a thermally activated behavior of the Arrhenius type, indicating that the conductance vanishes only at zero temperature.

*System and methods.*—We consider a two-dimensional quantum fluid of interacting bosons of mass  $m$  at temperature  $T$  subjected to a disordered potential  $V(\mathbf{r})$ , governed by the Hamiltonian

$$H = \sum_i \left[ -\frac{\nabla_i^2}{2m} + V(\mathbf{r}_i) \right] + \sum_{i < j} u(\mathbf{r}_i - \mathbf{r}_j). \quad (1)$$

The properties of the short-range repulsive interaction potential  $u(r)$  used in ultracold-atom experiments can be accurately described by an  $s$ -wave pseudopotential with an effective coupling strength  $g$  [37,38]. The disordered potential we take is a correlated, isotropic, and continuous speckle potential, as realized by laser light diffusion through a ground-glass plate [23–25,32]. Its average value coincides with its standard deviation  $V_R$ , and its two-point

correlation function is a Gaussian of rms radius  $\sigma_R$  [39,40]. In the following, we consider an interaction strength  $\tilde{g} \equiv mg/\hbar^2 = 0.1$ , a fixed chemical potential  $\mu$ , and a correlation radius  $\sigma_R = \sqrt{5}\xi_0$ , where  $\xi_0 = \hbar/\sqrt{2m\mu}$  is the healing length in the absence of disorder. These are typical values realized in ultracold-atom experiments [23,24]. For instance, for  $^{87}\text{Rb}$  atoms the chosen chemical potential corresponds to  $\mu/k_B \approx 56$  nK and  $\sigma_R = 0.5$   $\mu\text{m}$ .

Our study is based on a fully *ab initio* path-integral quantum Monte Carlo (QMC) approach, which allows for unbiased calculations of equilibrium, finite-temperature properties of interacting bosons [41] in terms of a discretized path-integral representation using  $M$  time slices. We use the worm algorithm [42] to sample the grand-canonical partition function at inverse temperature  $\beta = 1/k_B T$ . Whereas disorder is taken into account at the level of the primitive approximation, the two-body interaction is treated in the pair-product approximation [41,43]. The two-particle propagator is derived by solving the *s*-wave scattering problem at high temperatures,  $\varepsilon^{-1} = Mk_B T$ , which yields

$$\langle \mathbf{r}|e^{-\varepsilon H_2}|\mathbf{r}'\rangle \simeq \frac{m}{4\pi\hbar^2\varepsilon} e^{-m|\mathbf{r}-\mathbf{r}'|^2/4\hbar^2\varepsilon} + \frac{\tilde{g}}{8\pi} \int_0^\infty dk k e^{-\varepsilon(\hbar^2 k^2/m)} \times [J_0(kr)Y_0(kr') + J_0(kr')Y_0(kr)], \quad (2)$$

where  $H_2$  is the Hamiltonian of the relative motion of two particles and  $\mathbf{r}$  and  $\mathbf{r}'$  are the relative coordinates at different times, whereas  $J_0$  and  $Y_0$  are Bessel functions of the first and second kind, respectively. Contributions of higher ( $l > 0$ ) partial waves to the two-particle density matrix are approximated by their noninteracting expressions. Here, we report results from simulations of up to  $N = 10^5$  particles in a box of linear extension  $L$  with periodic boundary conditions, averaged over  $\approx 40$  disorder realizations. The typical number of time slices used here varies from  $M = 16$  for weak disorder to  $M = 70$  for strong disorder amplitudes.

*Superfluid transition.*—We first study the superfluid to normal fluid transition in the presence of disorder. To elucidate the critical properties of this transition, we calculate the static superfluid susceptibility  $\chi_s = (1/L^2) \times \int d\mathbf{r} d\mathbf{r}' \langle \Psi^\dagger(\mathbf{r})\Psi(\mathbf{r}') \rangle$  and the field correlation function  $g_1(r) = \langle \Psi^\dagger(\mathbf{r})\Psi(0) \rangle$ , where  $\Psi$  is the field operator and  $\langle \dots \rangle$  denotes thermal and disorder average. In the superfluid phase of the clean system, the decay of field correlations is algebraic,  $g_1(r) \sim r^{-\eta}$ , and the superfluid susceptibility diverges as  $\chi_s \sim L^{2-\eta}$ . The exponent  $\eta$  is directly related to the superfluid density  $n_s$  as  $\eta = (mk_B T)/(2\pi\hbar^2 n_s)$ . In the normal phase, field correlations are exponentially suppressed,  $g_1(r) \sim e^{-r/\gamma}$ , and the susceptibility remains finite in the thermodynamic limit.

Analysis of our QMC data allows us to study both qualitatively and quantitatively the superfluid to normal transition in the presence of disorder (Fig. 1). The inset in Fig. 1 shows the superfluid susceptibility  $\chi_s$  as a function of the system size for various temperatures at intermediate disorder amplitude  $V_R/\mu = 0.3$ . For high temperatures [curves in the lower (light-orange) zone],  $\chi_s$  converges to a finite value,

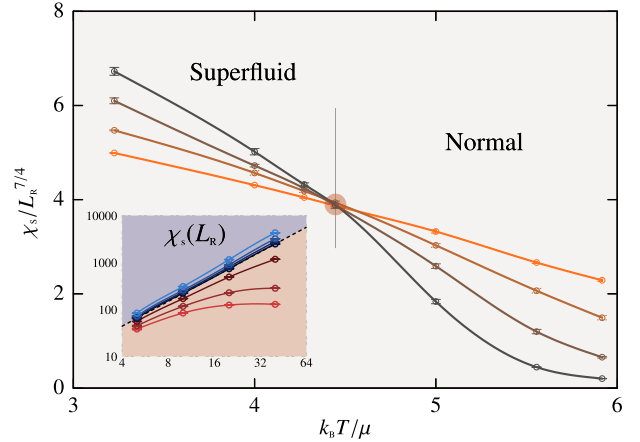


FIG. 1 (color online). Scaled superfluid susceptibility against temperature for system sizes in the range  $L_R = L/\sigma_R = 5-40$  at disorder strength  $V_R/\mu = 0.3$  and interaction strength  $\tilde{g} = 0.1$ . Darker curves mark increasingly large sizes. In the inset, the susceptibility is shown as a function of  $L_R$  (temperature increases from top to bottom). The divergence predicted by the BKT transition for clean systems ( $\eta = 1/4$ ) is indicated by the dashed line.

characteristic for the normal fluid phase. Above the critical temperature [curves in the upper (blue) zone],  $\chi_s$  shows an algebraic divergence. At the critical point, our QMC results are compatible with the scaling  $\chi_s \sim L^{7/4}$ , i.e.,  $\eta \simeq 1/4$ , as expected for the BKT transition in the clean system [12,13]. It is confirmed by the behavior of the rescaled superfluid susceptibility  $\chi_s/L^{7/4}$ , plotted in the main panel of Fig. 1 as a function of temperature for various values of  $L$ , where all curves cross nearly at a single point. Furthermore, our data for the superfluid density calculated from the winding number estimator [41] (not shown) are consistent with the universal jump at the transition temperature in the thermodynamic limit, expected for a BKT transition. We conclude that the superfluid transition of dirty bosons remains in the universality class of the clean BKT transition. To some extent, this result is expected for weak disorder. According to the Harris argument [14], local fluctuations of the disorder potential are smoothed out at the scale of the diverging correlation length at the BKT transition, thus introducing only a renormalization of the effective parameters. Our calculations show that it holds also for strong disorder (up to  $V_R \simeq \mu$ ).

The intersection point of the rescaled superfluid susceptibility (curves as in Fig. 1) precisely determines the transition temperature at fixed disorder amplitude. In our analysis, we find that the BKT scaling regime is attained for *increasingly large* system sizes, upon increasing the disorder strength. It results in a residual size dependence of the susceptibility intersection points. The latter is nonetheless well behaved and amenable for  $1/L$  extrapolation of the transition temperature in the thermodynamic limit. In order to have sufficiently small finite-size corrections to the BKT scaling, we use, for the largest disorder strength reported, systems of linear size  $L/\sigma_R \sim 40-80$ . These sizes should be contrasted with the typically (much)

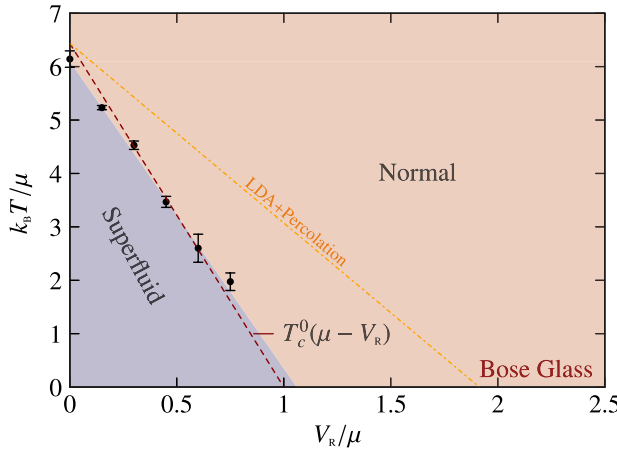


FIG. 2 (color online). Phase diagram of two-dimensional interacting bosons at fixed chemical potential and interaction strength  $\tilde{g} = 0.1$ . The dark dashed line is the critical temperature of the clean system with a renormalized chemical potential; the lighter dashed line is the prediction of a combination of LDA and percolation theory (see the text). For strong disorder, the normal system goes to the Bose-glass phase in the zero- $T$  limit.

smaller ones of the inner critical regions probed in experiments [6–8,23,24] and in some numerical simulations [44].

In Fig. 2, we show the resulting critical temperatures versus disorder strength and draw the superfluid to normal fluid phase diagram of dirty 2D bosons. Within numerical accuracy, the critical line is described by  $T_c(V_R) \simeq T_c^0(\mu - V_R)$ , where  $T_c^0 \simeq (\pi\mu)/(\tilde{g}k_B)/\log(13.2/\tilde{g})$  is the critical temperature for the disorder-free system [45]. The shift of the critical temperature can be understood in terms of the leading order renormalization of the chemical potential,  $\mu_c(V_R) - V_R = \mu_c(0)$ . For our parameters, upon increasing the disorder strength the critical density decreases from the disorder-free value  $n_c\sigma_R^2 \simeq 21$  to the zero-temperature ( $V_R \simeq \mu$ ) linearly extrapolated value of  $n_c\sigma_R^2 \simeq 7$ . At lower densities, the system remains normal for any of our temperatures,  $k_B T \gtrsim \mu$ , consistent with a Bose-glass phase at zero temperature, as indicated in Fig. 2.

We now compare our results to the possibility of a percolation-driven transition, as occurring in classical systems and investigated both experimentally [46] and theoretically [33] for 2D speckle disorder. In the superfluid phase, the Bose gas density for each realization of the disorder may be approximated by using the local density approximation (LDA):  $n_{\text{LDA}}(\mathbf{r}, V_R) = n_0[\mu - V(\mathbf{r})]$ , where  $n_0(\mu)$  is the density of the clean system at chemical potential  $\mu$ . The quantitative agreement between this approximation and our QMC results is reasonably good in the superfluid phase. We consider percolating clusters in which the local density stays everywhere higher than the critical density of the clean system, i.e.,  $n_{\text{LDA}}(\mathbf{r}, V_R) \geq (mk_B T)/(2\pi\hbar^2)\log(380/\tilde{g})$  [45]. The occurrence of such percolating superfluid clusters yields the dotted (orange) line reported in Fig. 2, which shows that the percolation scenario strongly overestimates the critical disorder strength. Superfluidity disappears, while there still exist large percolating clusters above the critical density

of the clean system. Notice that we have disregarded the weak penetration of the density into the disorder potential barriers due to the finite healing length in the superfluid phase [47]. However, this effect does not alter the above conclusions, since it would further raise the percolation line in Fig. 2.

*Transport properties.*—We now address the strongly disordered regime, where superfluid coherence is lost and disorder substantially affects mass transport. A long-debated issue is to understand whether interacting systems preserve Anderson-like localization properties, as found in the single-particle case [15–19]. At zero temperature, the conditions for a localized (Bose-glass) phase to exist have been established in seminal works [48,49]. At finite temperature, however, the existence of a perfectly insulating state, characterized by an exactly vanishing conductance ( $G_{\text{DC}} = 0$ ), is intrinsically more complex, and theoretically plausible scenarios have been put forward only recently. The *many-body localization* transition scenario [15,19] implies the existence of a critical temperature  $T_{\text{loc}}$  separating the perfect insulator behavior at low energies where  $G_{\text{DC}}(T < T_{\text{loc}}) = 0$  from a delocalized, diffusive phase with  $G_{\text{DC}}(T > T_{\text{loc}}) \neq 0$ . This transition, however, has not been directly observed in experiments and remains at the center of intense theoretical activity, for instance, in out-of-equilibrium phenomena [50–52].

In order to identify possible signatures of many-body localization at finite temperature, we have computed transport properties in the strongly disordered region. Such transport properties are traditionally addressed in disordered materials subjected to an external electric bias. They were recently shown to be also accessible in a new generation of ultracold-atom experiments [25].

To obtain the zero-frequency (dc) conductance within the QMC method, we compute the imaginary-time correlations of the density current operator along a given direction  $\alpha$ ,  $\Lambda_\alpha(\tau, q) = \langle J_\alpha(\tau, q)J_\alpha(0, -q) \rangle$ . It allows us to reconstruct the associated longitudinal conductance  $G_{\text{reg}}(\omega)$  [53] from numerical analytical continuation [54–56] of the Laplace transform [57]

$$\Lambda_\alpha(\tau, 0) = 2\hbar \int_{-\infty}^{+\infty} d\omega \frac{\exp(-\hbar\omega\tau)\omega}{1 - \exp(-\hbar\omega\beta)} G_{\text{reg}}(\omega). \quad (3)$$

Imaginary-time correlations of high statistical quality are essential for a reliable reconstruction of the dynamical response  $G_{\text{reg}}(\omega)$ . Direct estimators of current correlations successfully used for lattice simulations [58,59] present a diverging statistical error in the small imaginary-time step limit in continuum systems, preventing its use for numerical analytical continuation for our purposes. To overcome this serious problem, we introduce a novel estimator that significantly reduces the statistical error, making possible a reliable determination of the conductance. The key observation is that the imaginary-time derivatives of the correlations are well behaved in the small time-step limit  $\epsilon \rightarrow 0$  and that the imaginary-time integral of the correlation function is also well behaved and directly related to the superfluid

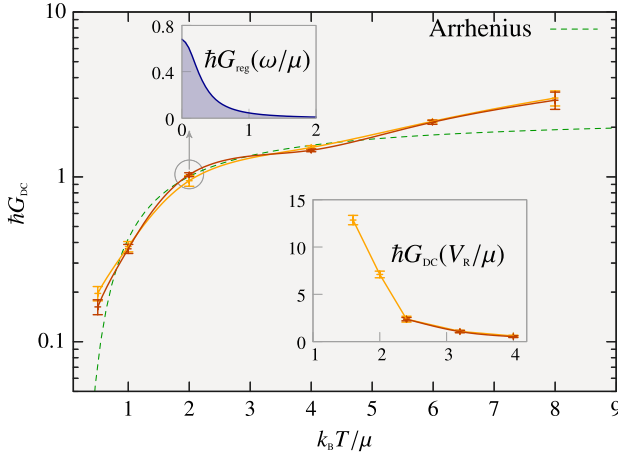


FIG. 3 (color online). Finite-temperature, zero-frequency longitudinal conductance for an intensity of the disorder  $V_R = 2.4 \mu$ . Error bars refer to averages over disorder, and the dashed line is a fit to a simple exponential Arrhenius law  $G_{\text{DC}}(T) \propto (\mu/k_B T)e^{-\Delta E/k_B T}$ . In the upper inset, the complete frequency dependence of the conductance is exemplified for  $k_B T = 2\mu$ . In the lower inset, the conductance at constant temperature ( $k_B T = \mu$ ) and varying disorder strength is also shown. In all cases, darker curves mark increasingly large sizes, in the range  $L/\sigma_R = 20-40$ .

density  $n_s$  [60]. We can therefore express the current-current correlations by means of the integral expression

$$\Lambda_\alpha(\tau, 0) = \frac{1}{\beta m} (n - n_s) + \int_0^\beta d\tau_1 \Lambda'_\alpha(\tau_1, 0) - \frac{1}{\beta} \int_0^\beta d\tau_1 \int_0^{\tau_1} d\tau_2 \Lambda'_\alpha(\tau_2, 0), \quad (4)$$

where the imaginary-time derivative of the correlation function reads

$$\begin{aligned} \varepsilon \Lambda'_\alpha(\tau, 0) &= \frac{1}{mL^2} \sum_i \langle [\nabla_i^\alpha V(\tau)] \times D^\alpha(0) \rangle \\ &- \frac{1}{2mL^2} \sum_{i,j,\beta} \langle D_j^\beta(\tau) \times [\nabla_i^\alpha \nabla_j^\beta V(\tau)] \times D^\alpha(0) \rangle + \mathcal{O}(\varepsilon^{3/2}). \end{aligned} \quad (5)$$

In the latter expression,  $\nabla_i^\alpha$  is the derivative with respect to the position of the  $i$ th particle,  $D^\alpha(\tau) = \sum_j^N D_j^\alpha(\tau) = \sum_j^N [R_j^\alpha(\tau) - R_j^\alpha(\tau - \epsilon)]$  is proportional to the imaginary-time displacement of the center of mass, and  $V(\tau)$  is a generic one-body potential which in our specific case is the disordered speckle potential.

We first study the behavior of the dc longitudinal conductance  $G_{\text{DC}} = G_{\text{reg}}(\omega = 0)$  versus the temperature deep in the strong disorder regime. The outcome is shown in the main panel of Fig. 3 for a fixed disorder strength  $V_R = 2.4 \mu$ . The conductance decreases monotonically with temperature, a behavior which is typically observed in related experiments with disordered materials. In the zero-temperature limit, the longitudinal conductance is consistent with a vanishing value, as expected for the Bose-glass phase [49]. The overall behavior of  $G_{\text{DC}}$ , however, points towards a thermally activated transport (see the

fit in Fig. 3), at variance with a perfectly insulating, many-body localized phase at finite temperature, at least on the temperature scale accessible in our study. The energy broadening of the reconstructed dynamical conductances (see the upper inset in Fig. 3) remains finite and does not show any indication for a finite-temperature mobility edge.

In the lower inset in Fig. 3, we further show the behavior of the longitudinal conductance at fixed temperature versus the disorder strength  $V_R$ , ranging from the edge of the superfluid transition  $V_R \sim \mu$  to the strong disorder regime, with  $V_R \sim 4\mu$ . Compatibly with the thermally activated scenario, we find that the transport is exponentially suppressed with increasing disorder but never vanishes, in agreement with experimental results [25]. Size effects, though present, do not indicate any phase transition, at least for mesoscopic samples. Therefore, our *ab initio* analysis hints to a delocalized *bad Bose-metal* phase at finite temperature.

**Conclusions.**—We have studied two-dimensional interacting bosons in the presence of a correlated disordered potential by using *ab initio* quantum Monte Carlo calculations. We have found that the disorder renormalizes the low-energy Hamiltonian in the neighborhood of the superfluid transition, but the critical line remains in the universality class of the Berezinskii-Kosterlitz-Thouless transition. It holds for arbitrary strong disorder up to the zero-temperature Bose-glass transition. Moreover, we have developed a new estimator for the conductance, which does not suffer from diverging statistical errors. Deep in the strong disorder regime, the mass transport exhibits a thermally activated behavior, and it is strictly suppressed only at zero temperature. It points towards the existence of a Bose bad-metal phase, as the finite-temperature precursor of the Bose-glass insulator. We have found no indication of a finite-temperature many-body localization transition. Our results provide new theoretical insights both in the general understanding of disordered interacting systems and in the interpretation of experiments with both ultracold atoms and disordered materials.

We acknowledge discussions with B. Altshuler, D. Basko, T. Bourdel, T. Giamarchi, T. Roscilde, S. Moroni, and T. Ziman. This research was supported by the European Research Council (FP7/2007-2013 Grant Agreement No. 256294), Ministère de l’Enseignement Supérieur et de la Recherche, and Agence Nationale de la Recherche (“DisorderTransitions”). It was performed by using HPC resources from GENCI-CCRT/CINES (Grants No. t2012056853 and No. t2013056853). Use of the computing facility cluster GMPCS of the LUMAT federation (FR LUMAT 2764) is also acknowledged. Our simulations make use of the ALPS [61] scheduler library and statistical analysis tools [62–64].

- 
- [1] E. Abrahams, S. V. Kravchenko, and M. P. Sarachik, *Rev. Mod. Phys.* **73**, 251 (2001).
  - [2] L. A. Tracy, E. H. Hwang, K. Eng, G. A. Ten Eyck, E. P. Nordberg, K. Childs, M. S. Carroll, M. P. Lilly, and S. Das Sarma, *Phys. Rev. B* **79**, 235307 (2009).

- [3] G. Allison, E. A. Galaktionov, A. K. Savchenko, S. S. Safonov, M. M. Fogler, M. Y. Simmons, and D. A. Ritchie, *Phys. Rev. Lett.* **96**, 216407 (2006).
- [4] P. A. Crowell, F. W. Van Keuls, and J. D. Reppy, *Phys. Rev. Lett.* **75**, 1106 (1995).
- [5] P. A. Crowell, F. W. Van Keuls, and J. D. Reppy, *Phys. Rev. B* **55**, 12 620 (1997).
- [6] D. R. Luhman and R. B. Hallock, *Phys. Rev. Lett.* **93**, 086106 (2004).
- [7] D. R. Luhman and R. B. Hallock, *Phys. Rev. B* **74**, 014510 (2006).
- [8] R. J. Lazarowich and P. Taborek, *Phys. Rev. B* **74**, 024512 (2006).
- [9] S.H. Pan *et al.*, *Nature (London)* **413**, 282 (2001).
- [10] N.D. Mermin and H. Wagner, *Phys. Rev. Lett.* **17**, 1133 (1966).
- [11] P.C. Hohenberg, *Phys. Rev.* **158**, 383 (1967).
- [12] V.L. Berezinskii, Sov. Phys. JETP **34**, 610 (1972).
- [13] J.M. Kosterlitz and D.J. Thouless, *J. Phys. C* **6**, 1181 (1973).
- [14] A.B. Harris, *J. Phys. C* **7**, 1671 (1974).
- [15] D. Basko, I. Aleiner, and B. Altshuler, *Ann. Phys. (N.Y.)* **321**, 1126 (2006).
- [16] V. Oganesyan and D.A. Huse, *Phys. Rev. B* **75**, 155111 (2007).
- [17] P. Lugan, D. Clément, P. Bouyer, A. Aspect, and L. Sanchez-Palencia, *Phys. Rev. Lett.* **99**, 180402 (2007).
- [18] P. Lugan and L. Sanchez-Palencia, *Phys. Rev. A* **84**, 013612 (2011).
- [19] I.L. Aleiner, B.L. Altshuler, and G.V. Shlyapnikov, *Nat. Phys.* **6**, 900 (2010).
- [20] L. Sanchez-Palencia and M. Lewenstein, *Nat. Phys.* **6**, 87 (2010).
- [21] Z. Hadzibabic, P. Kruger, M. Cheneau, B. Battelier, and J. Dalibard, *Nature (London)* **441**, 1118 (2006).
- [22] R. Desbuquois, L. Chomaz, T. Yefsah, J. Léonard, J. Beugnon, C. Weitenberg, and J. Dalibard, *Nat. Phys.* **8**, 645 (2012).
- [23] M. C. Beeler, M. E. W. Reed, T. Hong, and S. L. Rolston, *New J. Phys.* **14**, 073024 (2012).
- [24] B. Allard, T. Plisson, M. Holzmann, G. Salomon, A. Aspect, P. Bouyer, and T. Bourdel, *Phys. Rev. A* **85**, 033602 (2012).
- [25] S. Krinner, D. Stadler, J. Meineke, J.-P. Brantut, and T. Esslinger, *Phys. Rev. Lett.* **110**, 100601 (2013).
- [26] F. Alet and E.S. Sørensen, *Phys. Rev. E* **67**, 015701 (2003).
- [27] N. Prokof'ev and B. Svistunov, *Phys. Rev. Lett.* **92**, 015703 (2004).
- [28] G.M. Wysin, A.R. Pereira, I.A. Marques, S.A. Leonel, and P.Z. Coura, *Phys. Rev. B* **72**, 094418 (2005).
- [29] S.G. Söyler, M. Kiselev, N.V. Prokof'ev, and B.V. Svistunov, *Phys. Rev. Lett.* **107**, 185301 (2011).
- [30] F. Lin, E.S. Sørensen, and D.M. Ceperley, *Phys. Rev. B* **84**, 094507 (2011).
- [31] J.P. Álvarez Zúñiga and N. Laflorencie, [arXiv:1304.7636](https://arxiv.org/abs/1304.7636).
- [32] D. Clément, A.F. Varón, J.A. Retter, L. Sanchez-Palencia, A. Aspect, and P. Bouyer, *New J. Phys.* **8**, 165 (2006).
- [33] L. Pezzé, M. Robert-de-Saint-Vincent, T. Bourdel, J.-P. Brantut, B. Allard, T. Plisson, A. Aspect, P. Bouyer, and L. Sanchez-Palencia, *New J. Phys.* **13**, 095015 (2011).
- [34] S. Pilati, S. Giorgini, and N. Prokof'ev, *Phys. Rev. Lett.* **102**, 150402 (2009).
- [35] S. Pilati, S. Giorgini, M. Modugno, and N. Prokof'ev, *New J. Phys.* **12**, 073003 (2010).
- [36] T. Bourdel, *Phys. Rev. A* **86**, 063626 (2012).
- [37] D.S. Petrov, M. Holzmann, and G.V. Shlyapnikov, *Phys. Rev. Lett.* **84**, 2551 (2000).
- [38] The effective two-dimensional coupling parameter in the ultracold-atom experiment reads  $g = \sqrt{8\pi(a_s/a_z)(\hbar^2/m)}$ , where  $a_s$  is the three-dimensional  $s$ -wave scattering length and  $a_z = \sqrt{\hbar/m\omega_z}$  is the characteristic trapping length in the transverse direction.
- [39] J. Goodman, *Speckle Phenomena in Optics: Theory and Applications* (Roberts and Company, Greenwood Village, CO, 2007).
- [40] The disordered potential is obtained as the square modulus of the discrete Fourier transform of  $(\sqrt{2\pi V_R}/\tilde{\sigma}L) \times \exp[-(k_x^2 + k_y^2)/(4\tilde{\sigma}^2) + i\theta(k_x, k_y)]$ , where  $\tilde{\sigma}^2 = (1/2\sigma_R^2)$ ,  $\theta(k_x, k_y)$  is an uniformly distributed random phase, and  $L$  is the linear size of the two-dimensional system. The wave vectors are integer multiples of  $\Delta k = 2\pi/L$ , and we typically take  $\sim 10^4$  wave vectors along each spatial direction.
- [41] D.M. Ceperley, *Rev. Mod. Phys.* **67**, 279 (1995).
- [42] M. Boninsegni, N. Prokof'ev, and B. Svistunov, *Phys. Rev. Lett.* **96**, 070601 (2006).
- [43] W. Krauth, *Phys. Rev. Lett.* **77**, 3695 (1996).
- [44] G.E. Astrakharchik, K.V. Krutitsky, and P. Navez, *Phys. Rev. A* **87**, 061601(R) (2013).
- [45] N. Prokof'ev, O. Ruebenacker, and B. Svistunov, *Phys. Rev. Lett.* **87**, 270402 (2001).
- [46] L.N. Smith and C.J. Lobb, *Phys. Rev. B* **20**, 3653 (1979).
- [47] L. Sanchez-Palencia, *Phys. Rev. A* **74**, 053625 (2006).
- [48] T. Giamarchi and H.J. Schulz, *Phys. Rev. B* **37**, 325 (1988).
- [49] M.P.A. Fisher, P.B. Weichman, G. Grinstein, and D.S. Fisher, *Phys. Rev. B* **40**, 546 (1989).
- [50] E. Canovi, D. Rossini, R. Fazio, G.E. Santoro, and A. Silva, *Phys. Rev. B* **83**, 094431 (2011).
- [51] G. Carleo, F. Becca, M. Schiro, and M. Fabrizio, *Sci. Rep.* **2**, 243 (2012).
- [52] E. Canovi, D. Rossini, R. Fazio, G.E. Santoro, and A. Silva, *New J. Phys.* **14**, 095020 (2012).
- [53] Notice that we refer here to mass transport. The conventional electric conductance is  $\tilde{G}_{\text{reg}}(\omega) = q^2 G_{\text{reg}}(\omega)$  for particles of charge  $q$ .
- [54] A.W. Sandvik, *Phys. Rev. B* **57**, 10287 (1998).
- [55] J.E. Gubernatis, M. Jarrell, R.N. Silver, and D.S. Sivia, *Phys. Rev. B* **44**, 6011 (1991).
- [56] G. Carleo, S. Moroni, and S. Baroni, *Phys. Rev. B* **80**, 094301 (2009).
- [57] R. Kubo, *Rep. Prog. Phys.* **29**, 255 (1966).
- [58] D.J. Scalapino, S.R. White, and S. Zhang, *Phys. Rev. B* **47**, 7995 (1993).
- [59] N. Trivedi, R.T. Scalettar, and M. Randeria, *Phys. Rev. B* **54**, R3756 (1996).
- [60] E.L. Pollock and D.M. Ceperley, *Phys. Rev. B* **36**, 8343 (1987).
- [61] <http://alps.comp-phys.org/>.
- [62] M. Troyer, B. Ammon, and E. Heeb, *Lect. Notes Comput. Sci.* **1505**, 191 (1998).
- [63] A. Albuquerque *et al.*, *J. Magn. Magn. Mater.* **310**, 1187 (2007).
- [64] B. Bauer *et al.*, *J. Stat. Mech.* (2011) P05001.